Article

Determination of the [^{15}N]-Nitrate/[^{14}N]-Nitrate Ratio in Plant Feeding Studies by GC–MS

Sebastian Schramm, Maria Fe Angela Comia Boco, Sarah Manzer, Oliver König, Tong Zhang, Fatima Tuz Zohora Mony, Adebimpe Nafisat Adedeji-Badmus, Brigitte Poppenberger and Wilfried Rozhon *

Biotechnology of Horticultural Crops, TUM School of Life Sciences Weihenstephan, Technical University of Munich, Liesel-Beckmann-Straße 1, 85354 Freising, Germany; seb.schramm@tum.de (S.S.); mariafefeangela.boco@studio.unibo.it (M.F.A.C.B.); sarah.manzer@tum.de (S.M.); oliver.koenig@tum.de (O.K.); ge52qug@mytum.de (T.Z.); fatima.mony@tum.de (F.T.Z.M.); adebimpe.adedeji@tum.de (A.N.A.-B.); brigitte.poppenberger@wzw.tum.de (B.P.)

* Correspondence: wilfried.rozhon@wzw.tum.de; Tel.: +49-8161-71-2023

Abstract: Feeding experiments with stable isotopes are helpful tools for investigation of metabolic fluxes and biochemical pathways. For assessing nitrogen metabolism, the heavier nitrogen isotope, [^{15}N], has been frequently used. In plants, it is usually applied in form of [^{15}N]-nitrate, which is assimilated mainly in leaves. Thus, methods for quantification of the [^{15}N]-nitrate/[^{14}N]-nitrate ratio in leaves are useful for the planning and evaluation of feeding and pulse–chase experiments. Here we describe a simple and sensitive method for determining the [^{15}N]-nitrate to [^{14}N]-nitrate ratio in leaves. Leaf discs (8 mm diameter, approximately 10 mg fresh weight) were sufficient for analysis, allowing a single leaf to be sampled multiple times. Nitrate was extracted with hot water and derivatized with mesitylene in the presence of sulfuric acid to nitromesitylene. The derivatization product was analyzed by gas chromatography–mass spectrometry with electron ionization. Separation of the derivatized samples required only 6 min. The method shows excellent repeatability with intraday and interday standard deviations of less than 0.9 mol%. Using the method, we show that [^{15}N]-nitrate declines in leaves of hydroponically grown *Crassocephalum crepidioides*, an African orphan crop, with a biological half-life of 4.5 days after transfer to medium containing [^{14}N]-nitrate as the sole nitrogen source.

Keywords: GC–MS; mesitylene; nitrate; nitrogen; feeding experiments; stable isotope

1. Introduction

Nitrogen represents a very important fraction of a plant's chemical composition. It is an essential plant macro-nutrient, necessary to ensure correct development and growth. Nitrogen is a fundamental constituent of amino acids, the building blocks of peptides and proteins. It is present in chlorophyll, a crucial molecule in photosynthesis, and in the phytohormones auxin and cytokinin. In addition, nitrogen is a constituent of the nucleobases present in DNA, RNA, and in many co-substrates, for instance ATP (adenosine triphosphate), NADH (nicotinamide adenine dinucleotide), and UDP-glucose (uridine diphosphate glucose), involved in a tremendous number of metabolic processes. It is also present in polyamines, quaternary ammonium compounds [1], plant defense compounds including alkaloids [2–5], glucosinolates [6,7], benzoxazinoids [8], some phytoalexins [9], and in many other metabolites. Plants grown in nitrogen-rich substrates may contain more than 5% nitrogen in dry weight while plants grown under nitrogen-limiting conditions contain still approximately 0.5–1.0% nitrogen in dry weight [10,11]. Plants take up nitrogen via the root system mainly in form of nitrate and ammonium. In most substrates

nitrate is the predominant form but ammonium may be present at high levels in flooded soils [12] and in grasslands [13]. Ammonium can be incorporated directly in the root into amino acids or under some conditions, particularly at a high supply, may be transported to the shoot [14,15]. In contrast, nitrate is mainly transported to the shoot and reduced by nitrate reductase to nitrite, which is in turn further reduced by nitrite reductase to ammonium. Ammonium is incorporated by the actions of glutamine synthetase and glutamate synthetase into glutamine and glutamate [16], respectively, which serve as precursors for biosynthesis of further amino acids [17] and other nitrogen-containing compounds. Since ammonium [18–20] and nitrite [21] are toxic for plant tissues, nitrate reduction is well regulated [22–24] to avoid accumulation of these intermediates. Consequently, nitrate may accumulate in leaves under rich fertilization.

Sufficient nitrogen supply is crucial for high plant biomass production and yield, which has been studied in many plant species including the cereals wheat [25,26], maize [27–29], oat [30], and barley [31,32], oilseeds like canola [25] and sunflower [33], root crops like potato [34,35] and sugar beet [36], vegetables including spinach [37], lettuce [10], and kohlrabi [11] and energy crops like willow [38] and *Miscanthus sinensis* [39]. Even the legumes, which possess root nodules that contain nitrogen-fixing symbionts, show increased yields when grown in nitrate-rich substrates [40,41]. However, fertilizers must be applied at the demand of the plants since overfertilization causes severe environmental problems including contamination of surface and groundwater with nitrate [42] and is responsible for algal bloom in the sea [43]. In addition, overfertilization of vegetables like lettuce, spinach, celery, and Chinese cabbage causes nitrate accumulation at levels of up to several g/kg fresh weight [44–47]. Possible health impacts of a high dietary intake of nitrate are intensively and controversially discussed [48–55].

Due to the importance of nitrate, a number of methods have been developed for quantification of nitrate in soils, growth substrates and samples from plants, animals, and humans. These methods include spectrophotometry [56,57], ion sensitive electrode [58], ion chromatography [59], ion-pair chromatography [60], gas chromatography [61], and capillary electrophoresis [62]. In addition, soluble nitrogen-containing compounds, particularly the amino acids, can be quantified in plant tissues for assessing the nutritional status of plants and ripening of fruits [63–66]. While these methods are useful for evaluating plant nutritional status, they are of limited use for investigation of nitrogen fluxes in plants. Metabolic fluxes are often investigated by so called pulse–chase analysis, where organisms or cells are initially incubated with a labeled compound (the pulse), which will be incorporated into the metabolites. Subsequently, the labeled compound is removed and replaced by the unlabeled version. Depletion of the labeled molecule and its conversion to labeled metabolites is measured over time during the so called 'chase' period. Due to their simple detection, classically radio isotopes were used for such experiments. In case of nitrogen, the radionuclide ^{13}N has been used for tracer studies [14,67–69]. However, the short ^{13}N half-life of 9.97 min [70] is a drawback since ^{13}N must be produced on site. Alternatives to radionuclides include stable isotopes, which also allow for performing field studies. The two stable isotopes of nitrogen are ^{14}N, which has an abundance in the atmosphere of 99.634 mol%, and ^{15}N with an atmospheric abundance of only 0.366 mol% [71]. The huge difference in abundance makes ^{15}N a good tracer for metabolic studies. This technique has, for instance, been used to quantify nitrogen fixation [72], estimate the nitrogen flow in alfalfa plants [73], investigate nitrogen assimilation and amino acid translocation in barley [68,74,75], follow nitrogen remobilization from vegetative organs in pea [76], study nitrogen metabolism in buds of *Picea glauca* [77], and observe nitrogen fluxes in *Arabidopsis thaliana* seeds during the initiation of germination [78]. ^{15}N labeling is also useful for obtaining metabolites and proteins [79] accessible for NMR spectroscopy since the ^{15}N nucleus gives much sharper signals than the ^{14}N nucleus [77].

^{15}N contents can be analyzed by elemental analysis–isotope ratio mass spectrometry (EA–IRMS) [80,81], gas chromatography coupled to a combustion and reduction unit and a mass spectrometer [82], and by nuclear magnetic resonance spectroscopy (NMR) [77,78,83–85]. Other methods, including emission spectroscopy [86] and IR spectroscopy [87,88], are rarely used.

For feeding experiments with stable nitrogen isotopes [^{15}N]-potassium nitrate is most commonly used. For designing an appropriate experimental setup, the kinetics of replacement of [^{14}N]-nitrate by [^{15}N]-nitrate (or vice versa) in the plant tissue are relevant. The methods mentioned above measure either the total nitrogen content (EA-IRMS, emission spectroscopy), cannot analyze nitrate (nitrate is non-volatile and cannot be analyzed directly by GC), or lack insensitivity for analysis of small sample quantities (NMR) and are thus not suitable for rapid determination of the ratio of [^{15}N]-nitrate/[^{14}N]-nitrate in limited amounts of plant material.

Several methods for quantification of nitrate in biological samples, mainly of human or animal origin, using [^{15}N]-nitrate as an internal standard have been described. Green et al. presented a method for quantification of nitrate by spiking the sample with [^{15}N]-nitrate followed by reaction with benzene to nitrobenzene. The ratio of [^{14}N] and [^{15}N]-nitrobenzene was subsequently analyzed by gas chromatography–mass spectrometry (GC–MS) to determine the nitrate concentration [89]. Similar procedures using other, more reactive aromatic compounds were also developed [90–92]. Other methods made use of reaction of nitrate with pentafluorobenzyl bromide and subsequent GC–MS analysis of the obtained derivatives [93,94]. Here we tested whether these methods can be applied for determining the [^{15}N]-nitrate/[^{14}N]-nitrate ratio in plant material using GC–MS with electron impact ionization. We found that mesitylene gives the best results as the derivatization reagent. We optimized all the steps of the method including extraction, derivatization, and detection. Possible interferences with plant metabolites were investigated and finally the method was validated. The method presented can be a helpful tool for establishing appropriate conditions for ^{15}N feeding and pulse–chase experiments for measuring the level of stable isotope labeled nitrate in plants.

2. Results

Several GC–MS-based methods for quantification of nitrate in mammalian fluids, mainly urine, saliva, and plasma, have been reported. They depend on reaction of the nitrate ion with 2,3,4,5,6-pentafluorobenzyl bromide [93–96], benzene [89], 1,3,5-trimethoxybenzene [92], or mesitylene [90,91] to form organic compounds, which can be sensitively analyzed by GC–MS. 1,2,3,4,5-Pentafluorobenzyl bromide reacts with nucleophiles under mild conditions. Although nitrate is a poor nucleophile, it can substitute the bromine of 1,2,3,4,5-pentafluorobenzyl bromide to form a nitric acid ester. The other compounds mentioned above are nitrated via electrophilic aromatic substitution: nitrate reacts first with sulfuric acid to the nitronium cation, which subsequently combines with the aromatic ring to yield the nitrated aromatic compounds (Figure 1A). In that case nitrogen is directly linked to carbon and the obtained derivatives are very stable, which makes them highly suitable for quantification. The reaction is very specific for nitrate; the only side reaction that may happen is sulfonation of the aromatic reagent. Since the nitro group has a strong inactivating effect on the aromatic system, double derivatization is not observed. Among the reagents mentioned above, 1,3,5-trimethoxybenzene has, due to the activating effect of the methoxy groups, the highest reactivity. Mesitylene is, because of the methyl groups, slightly activated while benzene shows the lowest reactivity among these reagents.

To test the suitability of these reagents for determination of the [^{15}N]/[^{14}N]-nitrate ratio in plant leaves by GC–EI–MS (gas chromatography–electron ionization–mass spectrometry), test reactions were performed. Reaction products obtained with 1,3,5-trimethoxybenzene contained high levels of acid, probably sulfonated reagent, and were thus unfavorable for analysis by GC–MS. Tests with 2,3,4,5,6-pentafluorobenzyl bromide revealed that only fragments with *m/z* 181 and 161 were visible in the positive EI–MS spectrum. These ions had both lost the nitrogen and were therefore not suitable for distinguishing [^{14}N] and [^{15}N]-nitrate. This is in accordance with the literature, where 2,3,4,5,6-pentafluorobenzyl derivatives are usually analyzed by MS after electron capture negative ion chemical ionization [93,96–98]. In addition, 2,3,4,5,6-pentafluorobenzyl bromide reacts also with many other compounds typically present in plants, for instance phenolics [99] and fatty acids [98]. In contrast, mesitylene gave very promising results: a peak at *m/z* 148 was obtained for [^{14}N]-nitrate (Figure 1B).

The small peak at *m/z* 149 with a height of approximately 10% of the *m/z* 148 peak originates from the natural abundance of the ^{13}C and ^{15}N isotopes. The observed fragmentation pattern indicated that the ionized molecule with an *m/z* of 165 reacted under loss of a hydroxyl radical to the base ion *m/z* 148, which reacted further under loss of carbon monoxide to *m/z* 120. The latter ion decayed under loss of hydrogen cyanide to *m/z* 93. This is in agreement with the fragmentation pattern observed for ^{15}N-nitrate, where peaks of *m/z* 149 and 121, one mass unit higher than the ^{14}N-containing ions, were observed. In addition, also for ^{15}N-nitrate *m/z* 93 was observed, confirming that this ion does not contain nitrogen.
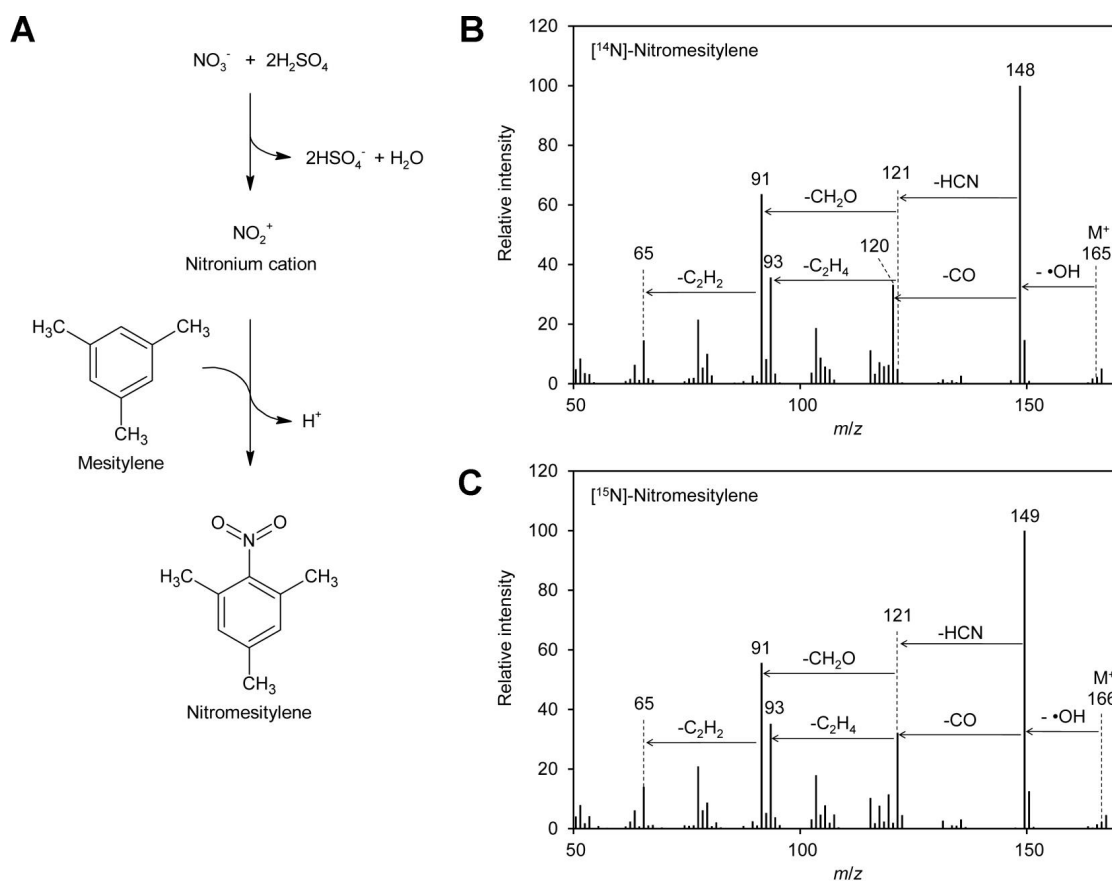

Figure 1. Formation of nitromesitylene and MS spectra. (**A**) Nitrate reacts with sulfuric acid to the nitronium cation, which reacts subsequently with mesitylene to form nitromesitylene. (**B**) EI–MS spectrum of ^{14}N-nitromesitylene. Neutral losses of a hydroxyl radical (·OH), carbon monoxide (CO), and hydrogen cyanide (HCN) are indicated. (**C**) EI–MS spectrum of ^{15}N-nitromesitylene. Original data are presented in Supplementary File S1.

For benzene, the molecular peak M $^+$ of *m/z* 123 obtained by derivatization of ^{14}N-nitrate and of *m/z* 124 for ^{15}N-nitrate dominated the spectra (Figure 2). However, also [MH] $^+$ showed a significant peak and thus the molecular peak was not suitable for determination of the ^{15}N/^{14}N-nitrate ratio. Apart from the molecular peak only the fragments *m/z* 107 (for ^{14}N) and *m/z* 108 for (^{15}N) were found to be suitable for determining the ^{15}N/^{14}N-nitrate ratio since all other fragments lacked nitrogen. However, this signal is relatively weak. In addition, nitrobenzene also shows peak tailing and the reagent benzene is toxic and carcinogenic [100]. Thus, benzene is clearly less suitable than mesitylene.

Taking these results together, mesitylene might be a useful reagent for simple determination of the ^{15}N/^{14}N-nitrate ratio in plants. Thus, we decided to focus on optimizing the reaction and analysis conditions for this reagent.
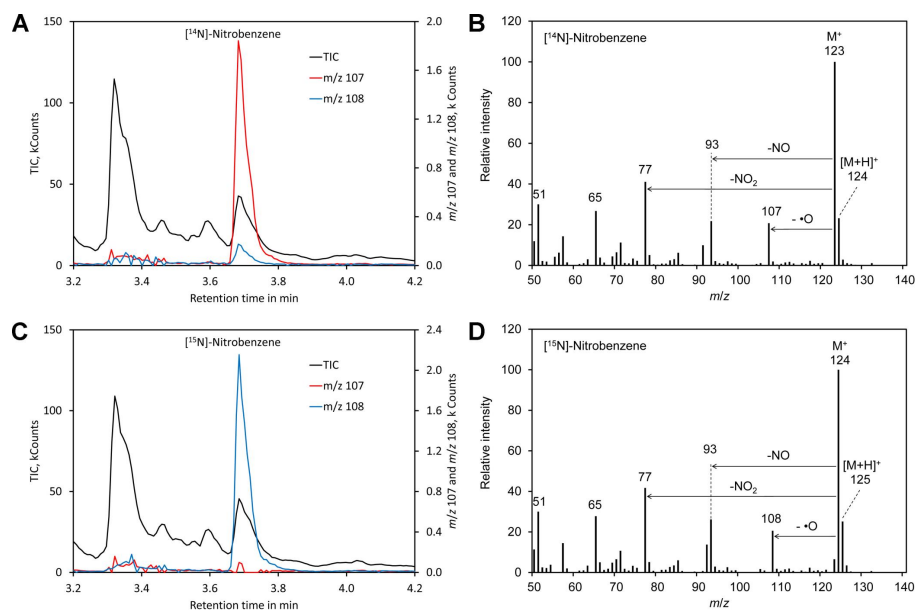
Figure 2. Derivatization with benzene. (**A**) Chromatogram obtained by derivatization of [^{14}N]-nitrate. (**B**) Mass spectrum of the derivatization product [^{14}N]-nitrobenzene. (**C**) Chromatogram obtained by derivatization of [^{14}N]-nitrate. (**D**) Mass spectrum of the derivatization product [^{14}N]-nitrobenzene. Original data are included in Supplementary File S2.

2.1. Method Development

Formation of the nitronium cation, the first step in nitration of mesitylene (Figure 1A), depends on the sulfuric acid concentration. Thus, the reaction was performed in the presence of 65–85% (*w/w*) sulfuric acid. In addition, the reaction time was varied between 5 and 20 min. A possible side reaction to nitration of the aromatic ring is oxidation of the methyl residues, which happens particularly at an elevated temperature [101,102]. Thus, the reactions were performed at room temperature. Since the mixture was biphasic, the tubes were shaken vigorously to enhance the reaction. For reliable quantification of the reaction product nitromesitylene, 2,4-dinitrotoluene (DNT) was added to the reaction. DNT is a suitable internal standard because the presence of two nitro groups deactivates the aromatic system and thus DNT does not react with nitrate under the conditions tested here. In addition, DNT was well separated from nitromesitylene by GC–MS and the fragment with *m/z* 165 can be used for quantification (Figure 3). However, DNT showed significant peak tailing. Since DNT was only needed during optimization of the method, the drawback of DNT peak tailing was considered as acceptable. In the final method DNT is not added to the samples and thus DNT peak tailing has no impact on the accuracy of [^{15}N]/[^{14}N]-nitrate ratio measurements.
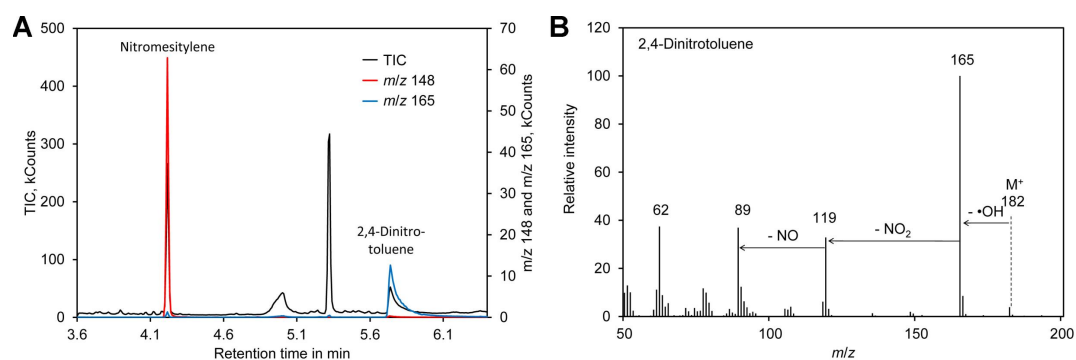

Figure 3. 2,4-Dinitrotoluene as internal standard. (**A**) Chromatogram obtained by derivatization of [^{14}N]-nitrate with nitromesitylene containing 0.5 mM 2,4-dinitrotoluene. (**B**) Mass spectrum of 2,4-dinitrotoluene. Original data are included in Supplementary File S3.

A clear increase of the nitromesitylene signal was observed with the concentration of sulfuric acid (Figure 4A). At 65% and 70% no reaction was observed while little product was formed at 75%. For the 10 min and 20 min reactions the maximum was reached at 80% sulfuric acid and no further increase of the signal was observed when 85% sulfuric acid was used. For the 5 min reactions, the maximum was observed only for 85% sulfuric acid although a high yield was also obtained at 80%. These data indicate that a sulfuric acid concentration of at least 80% and a reaction time of 10 to 20 min should be used. The obtained reaction product was quite acidic since a lot of carbon dioxide was evolved when the supernatant was treated with sodium carbonate. A possible explanation might be that some sulfuric acid had dissolved in mesitylene. Experiments showed that this problem can be eliminated by addition of water to the tubes after finishing the reactions. To enhance visibility of the phases a small amount of indigo carmine (approximately 0.01%) was added to the water used for dilution of the reaction mix, which stained the lower water/sulfuric acid phase intensively blue while the upper organic phase remained colorless.
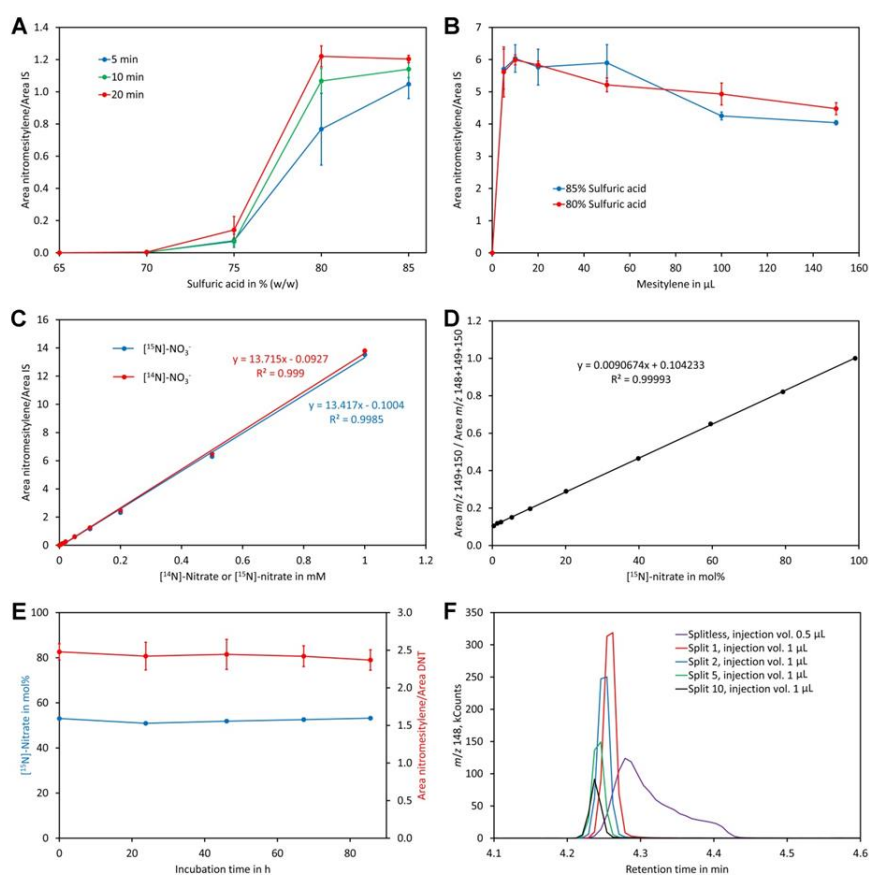

Figure 4. Optimization of the method. (**A**) Reaction time and sulfuric acid concentration. The dots and bars are the average and SD of three replicates, respectively. (**B**) Amount of mesitylene and sulfuric acid concentration. The dots and bars are the average and SD of three replicates, respectively. (**C**) Linearity in the range of 0 to 1 mM [^{14}N]-nitrate and [^{15}N]-nitrate. (**D**) Calibration curve for determination of the [^{15}N]-nitrate level using standards containing 0.2 mM nitrate. (**E**) Stability of the reaction product. The derivatized sample was injected after incubation for the indicated time. The blue dots represent the measured content of [^{15}N]-nitrate in mol% while the red dots represent the ratio of the area of nitromesitylene to the area of the internal standard 2,4-dinitrotoluene (DNT). The dots and bars are the average and SD of five measurements, respectively. (**F**) Testing different injection modes. The same sample was injected splitless or with a split ratio of 1, 2, 5, or 10. The injection volume was 1 μL except for splitless injection, where 0.5 μL was injected. Original data are presented in Supplementary File S4.

For the former experiments, pure mesitylene was used, which served on one hand as reagent and on the other hand as solvent. Mesitylene has a similar boiling point to the reaction product and thus only small volumes could be injected to prevent significant peak broadening of the nitromesitylene peak. In addition, pipette tips were almost invisible since their refractive index (approximately 1.49) is very similar to that of mesitylene (1.499). These disadvantages raised the question whether the amount of mesitylene may be downsized. Reactions with different volumes indicated that the highest signal was obtained with 10 µL mesitylene (the total volume of the organic phase was kept constant at 200 µL by adding heptane after incubation at room temperature for 20 min). At higher volumes, the signal decreased slightly (Figure 4B). Using 80% or 85% sulfuric acid had no significant effect on the reaction. Thus, 80% sulfuric acid and 10 µL mesitylene with a reaction time of 20 min and subsequent addition of water (containing indigo carmine) and 190 µL heptane for extraction of the reaction product were the most suitable conditions. Addition of heptane had also the advantage that pipette tips were well visible in the mesitylene/heptane mixture.

Reactions with different concentrations of nitrate showed perfect linearity for [14N]-nitrate and [15N]-nitrate and, importantly, an identical detector response (Figure 4C). Also, calibration curves for analysis of the level of [15N]-nitrate were linear when mol% [15N]-nitrate was plotted on the x-axis and the sum of the intensities of m/z 149 + 150 divided by the sum of the intensities of m/z 148 + 149 + 150 plotted on the y-axis (Figure 4D). The ion with m/z 150 had to be included to correct for nitrate that had reacted with mesitylene containing a [13C] atom. Without considering ion m/z 150, a polynomial function of second order rather than a linear function was obtained as a calibration curve.

To investigate the stability of the reaction product a sample was derivatized and analyzed immediately as well as on the following four days. The calculated ratio of [15N]-nitrate to [14N]-nitrate given in mol% [15N]-nitrate (Figure 4E) as well as the ratio of the peak areas of the reaction product nitromesitylene to the internal standard DNT were stable over the entire time tested. This confirms that the reaction product is stable for at least 80 h.

Initial analyses performed in the splitless injection mode showed relatively broad nitromesitylene peaks with a long tail (Figure 4F). Overloading of the column could be excluded as a reason for peak asymmetry since injection of small volumes gave the same result. However, analyses performed in the split mode showed symmetric peaks even at low split ratios (Figure 4F). Thus, we decided to use an injection volume of 1 µL and a split ratio of 1. Under these conditions sharp symmetric peaks with an approximately equal peak area compared to splitless injection were obtained.

Separation could be achieved within 6 min using a VF-ms column, making the analysis quick. Chromatograms of standards and leaf samples looked almost identical and showed no peaks interfering with the nitromesitylene peak, confirming that the method is highly specific and suitable for analysis of leaf extracts (Figure 5).

Spiking experiments with plant extracts showed a matrix effect, particularly when samples with high levels of phenolic compounds were measured (Figure 6A). In the presence of 0.57 mM phenolic compounds (calculated as ferulic acid equivalents in the Folin–Ciocalteu assay) a reduction of the signal by approximately one third was observed. In the presence of high levels of phenolic compounds (3.51 mM ferulic acid equivalents) only approximately 20% of the signal intensity of the control was observed. Analysis of [15N]-nitrate and [14N]-nitrate showed that presence even of high phenolic levels had no effect on the mole fraction (Figure 6B). The matrix effect may be caused by reaction of nitrate with phenolic compounds in the presence of sulfuric acid. Phenolic compounds can be efficiently removed by treatment with activated charcoal [103,104]. The sample containing a high level of phenolic compounds was treated with two types of activated charcoal and with synthetic graphite. Quantification of the phenolic compounds after treatment with the adsorbents showed that both types of activated charcoal removed phenolics efficiently (>0.02 mM residue) while graphite removed only approximately half of the phenolics (1.91 mM after treatment). However, analysis showed that activated charcoal purchased from Merck reduced the matrix effect significantly while activated charcoal from Alfa Aeser and synthetic graphite had only a small effect (Figure 6A). This indicates that also other

compounds apart from the phenolics assayed with the Folin–Ciocalteu assay might be responsible for quenching of the signal. Treatment with the adsorbents resulted in significantly lower levels for [^{15}N]-nitrate (Figure 6B). Thus, such a treatment is unsuitable for analysis. Since the matrix lowered the signal but did not change the measured [^{15}N]-nitrate/[^{14}N]-nitrate we decided to use the plant extracts directly.
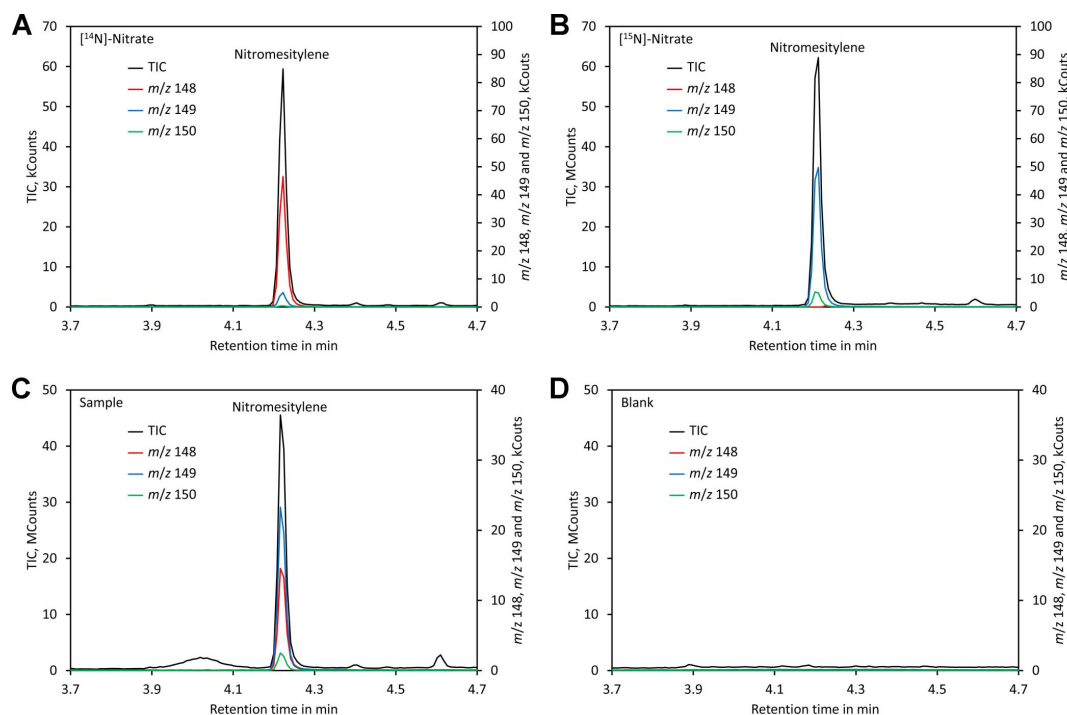

Figure 5. Chromatograms. (**A**) Chromatogram of a standard containing 0.2 mM [^{14}N]-nitrate. (**B**) Chromatogram of a standard containing 0.2 mM [^{15}N]-nitrate. (**C**) Chromatogram of a plant sample grown on medium containing [^{15}N]-nitrate and shifted to medium containing [^{14}N]-nitrate 3 days prior analysis. (**D**) Chromatogram of a blank. Original data are presented in Supplementary File S5.
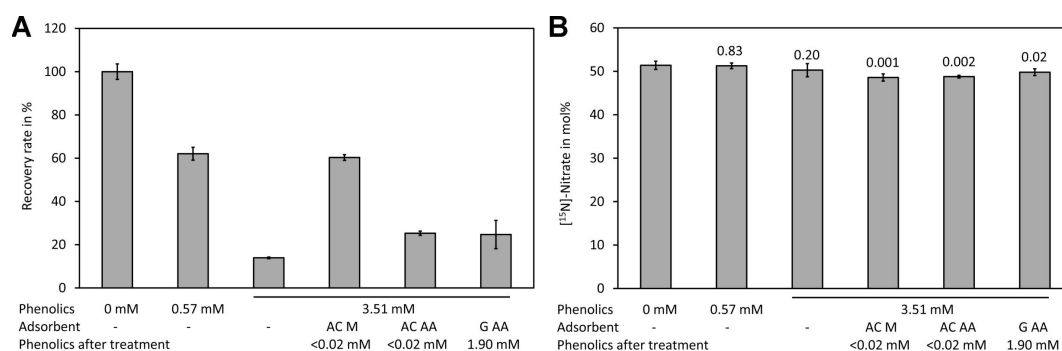

Figure 6. Matrix effect of plant leaf extracts. (**A**) Samples containing different levels of phenolic compounds (measured in mM ferulic acid equivalents) were spiked with a mixture containing [^{14}N]-nitrate and [^{15}N]-nitrate to a final concentration of 0.4 mM total nitrate and treated with the indicated adsorbents. Subsequently, the residual phenolics and the recovery rate of total nitrate were assayed using DNT as the internal standard. (**B**) The [^{15}N]-nitrate levels of the same samples shown in (**A**). Original data are presented in Supplementary File S6.

The results for [^{15}N]-nitrate presented above are the mole fraction in mol%. However, the mole fraction (x in mol%) and the ration (r in mol/mol) are connected via the formula [105]:

$$x = 100 * \frac{r}{1 + r} \tag{1}$$

Thus, if desired, the mole fraction can be converted to the ratio of [^{15}N]-nitrate to [^{14}N]-nitrate by using the formula:

$$r = \frac{x}{100 - x} \tag{2}$$

2.2. Method Validation

The limit of detection (LOD) and limit of quantification (LOQ) for [^{15}N]-nitrate in a mixture with [^{14}N]-nitrate were 0.65 mol% and 2.2 mol%, respectively. The sample used for determining the LOD and LOQ contained 0.2 mM nitrate since concentrations of 0.1 to 0.6 mM are typically seen for leaf extracts of *Crassocephalum crepidioides* (Supplementary File S7).

For assessing repeatability of the method two samples, one containing a medium and one a high level of phenolic compounds, were analyzed on five consecutive days with five replicates on each day. The calibration functions showed excellent linearity with Pearson correlation coefficients exceeding 0.999 on each day and excellent repeatability with relative standard deviations of 1.8% and 2.2% for the slope and interception, respectively (Table 1). Also, the results obtained for the sample containing a medium level of phenolics were highly repeatable with an intraday SD in the range of 0.25–0.81 mol% and an interday repeatability of 0.87 mol% (Table 2). The results for the sample with a high content of phenolics showed a slightly increased standard deviation with 0.51–2.27% for the intraday SD and 2.18 mol% for the interday SD. This can be explained by the lower signal and thus decreased signal to noise ratio.

Table 1. Interday repeatability of the calibration curve.

Experiments [1]	Calibration [2]		
	a	b	r
Day 1	0.00866	0.10698	0.99915
Day 2	0.00908	0.09956	0.99991
Day 3	0.00895	0.10065	0.99988
Day 4	0.00879	0.10223	0.99980
Day 5	0.00890	0.10155	0.99982
Average	0.00888	0.10220	
SD	0.00016	0.00286	
RSD in%	1.78	2.80	

[1] Original data are presented in Supplementary File S8; [2] Linear regression function of the type y = a × x + b; a, slope; b, interception; r, Pearson correlation coefficient.

Table 2. Intraday and interday repeatability.

Experiment [1]	Repeats	Reproducibility		
		Average mol%	SD mol%	RSD %
0.57 mM FA				
Day 1	5	53.10	0.57	1.07
Day 2	5	50.94	0.46	0.91
Day 3	5	51.99	0.25	0.48
Day 4	5	51.84	0.25	0.48
Day 5	5	51.33	0.81	1.58
Interday	25	51.84	0.88	1.70
3.51 mM FA				
Day 1	5	52.37	0.51	0.98
Day 2	5	48.75	2.27	4.65
Day 3	5	48.49	2.12	4.37
Day 4	5	49.86	0.99	1.99
Day 5	5	50.49	0.99	1.97
Interday	25	49.99	2.00	4.00

[1] Original data are presented in Supplementary File S8.

2.3. Application: Kinetics of [^{14}N]-Nitrate/[^{15}N]-Nitrate Replacement in Leaves of Crassocephalum crepidioides

To assess nitrate uptake of *Crassocephalum crepidioides*, an African orphan crop [4,106], plants were grown hydroponically in modified Hoagland medium containing [^{15}N]-nitrate as the sole nitrogen source. Since a closed system was used, water was regularly added to maintain a constant volume. In addition, samples were regularly analyzed for minerals and the medium was supplemented if required (Figure 7A). Nitrate and phosphate were the only minerals that had to be supplemented during the course of the experiment. After 29 days, the [^{15}N]-nitrate containing medium was replaced by [^{14}N]-nitrate medium and from this moment on leaf samples were taken for analysis of foliar [^{15}N]-nitrate and [^{14}N]-nitrate levels. Initially, a rapid decrease of [^{15}N]-nitrate was observed while at later time points a lower decline was observed. Regression analysis showed that [^{15}N]-nitrate decreased approximately exponentially with a biological half-life of 4.5 day (Figure 7B).
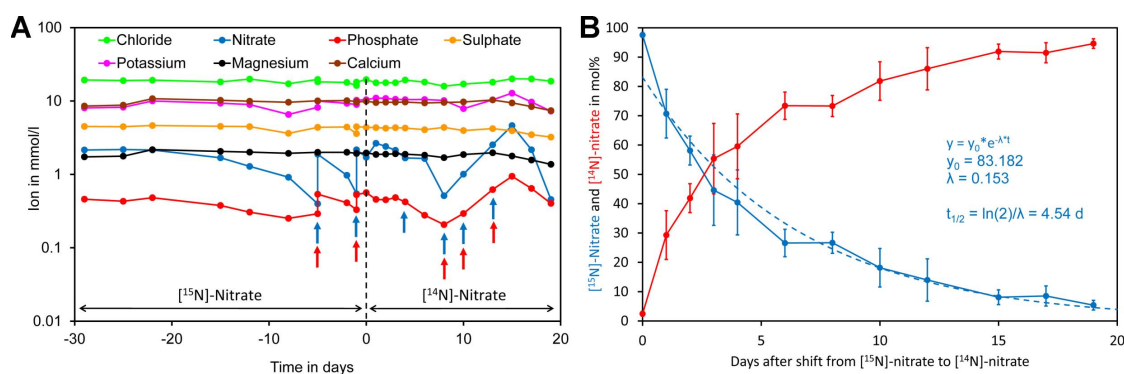

Figure 7. Kinetics of replacement of [^{15}N]-nitrate by [^{14}N]-nitrate in leaves of *Crassocephalum crepidioides*. (**A**) Plants were grown hydroponically in liquid medium containing [^{15}N]-nitrate as the sole nitrogen source for 29 days. Subsequently, the medium was replaced by medium containing [^{14}N]-nitrate as the sole nitrogen source (time 0, indicated by a dotted line) and grown for a further 19 days. Samples of the medium were taken at the indicated time points and analyzed for ions. If required, the medium was supplemented for nitrate by adding [^{15}N] or [^{14}N]-potassium nitrate (blue arrows) or for phosphate by adding potassium dihydrogen phosphate (red arrows). (**B**) Leaf disc samples were taken at the indicated time points for analysis of leaf [^{14}N]-nitrate and [^{15}N]-nitrate levels. The points and bars represent the biological average and standard error (SE) of samples taken from four different leaves. Total nitrate concentrations in leaf material and original data are presented in Supplementary Files S9 and S10.

3. Discussion

For assessing nitrogen metabolism and re-localization of nitrogen-containing metabolites, the heavier nitrogen isotope, ^{15}N, has been frequently used [68,72–78]. In plants it is usually applied in form of nitrate. Nitrate is assimilated mainly in leaves, where it is reduced via nitrite as the intermediate to ammonium, which is rapidly incorporated into amino acids [23,107]. Plants can accumulate high levels of nitrate, which can be critical for re-localization studies since it may take some time until the newly fed labeled nitrate has replaced the previously present unlabeled nitrate. Similarly, in pulse–chase experiments it is important to know to which extent the tracer nitrate has replaced the previously present species since that limits the extent of labeling in downstream metabolites. Thus, for appropriate planning of feeding and pulse–chase experiments knowledge of the kinetics of nitrate uptake and replacement of [^{15}N]-nitrate by [^{14}N]-nitrate (or vice versa) in leaves is very helpful.

The method for assessing the [^{15}N]-nitrate/[^{14}N]-nitrate in plant material described here is simple, rapid and does not require special equipment apart from a conventional GC–MS system with EI ionization. Nitrate is extracted with hot water and derivatized at room temperature with mesitylene in the presence of sulfuric acid to nitromesitylene. The reaction product is highly stable and the derivatized samples can be stored at room temperature for at least 80 h without any impact on the

performance. The calibration shows perfect linearity and the method is highly reproducible with intraday and interday SDs of less than 0.9 mol% for samples with moderate phenolic contents and less than 2.3 mol% for samples with high phenolic contents. Ideally, the nitrate concentration in the plant extract should be higher than 0.1 mM. At lower concentrations contamination with ubiquitously present nitrate might become critical. The limit of detection and quantification is 0.65 mol% and 2.2 mol% for [^{15}N]-nitrate, respectively. The reason for this relatively high detection limit is the natural abundance of ^{13}C of approximately 1.1%, which causes even in the absence of [^{15}N]-nitrate a signal at *m/z* 149 of approximately 10% of that at *m/z* 148, the ion obtained for derivatized [^{14}N]-nitrate. Opportunities to reduce the detection limit include using a high resolution mass spectrometer that can distinguish the mass defect of [^{15}N] and [^{13}C] or analyzing derivatized samples by gas chromatography coupled to combustion and reduction units and an isotope ratio mass spectrometer. However, for typical applications using isotope-enriched [^{15}N]-nitrate a normal GC–EI–MS system as used here is sufficient.

While the plant matrix had no effect on the results for the [^{15}N]-nitrate mole fraction, the signal intensity was significantly reduced, particularly in plant extracts containing high contents of phenolics. Experiments with activated charcoal showed that the matrix effect could be reduced. However, treatment with charcoal had a slight but significant impact on the results for the [^{15}N]-nitrate mole fraction. Thus, such a treatment was not useful. Interestingly, while charcoal treatment removed the phenolics as assessed by the Folin–Ciocalteu assay completely, the matrix effect was not completely eliminated. That indicates that the nitronium ion may also react with other compounds present in the plant extract apart from phenolics. Possible candidates are reducing compounds like ascorbic acid, glutathione, or cysteine [108,109]. However, since the measured [^{15}N]-nitrate mole fraction was not affected by the plant matrix this was not studied in more detail.

In summary, the presented method allows simple and reproducible determination of the foliar [^{15}N]-nitrate/[^{14}N]-nitrate ratio even from small samples. The method can be helpful for establishing and evaluating feeding and pulse–chase experiments.

4. Materials and Methods

4.1. Reagents

Potassium nitrate (>99%) was purchased from Duchefa (Haarlem, the Netherlands). [^{15}N]-Potassium nitrate (>98 isotope purity), mesitylene, heptane, indigo carmine, 2,4-dinitrotoluene, 1,3,5-trimethoxybenzene, toluene, 2,3,4,5,6-pentafluorobenzyl bromide, ethyl acetate, acetone, sodium tetraborate, and benzyldimethyltetradecylammonium chloride were purchased from Sigma (St. Louis, MO, USA). Sulfuric acid 96% and benzene were purchased from Carl Roth (Karlsruhe, Germany).

4.2. Plant Material and Growth Conditions

Crassocephalum crepidioides accession Ilé-Ifè [106] was used in this study. Seedlings were transplanted into hydroponic medium after 4 weeks of pre-cultivation on soil. Each hydroponic tank harbored 6 plants and contained 4 L of modified Hoagland medium with [^{15}N]-nitrate as the sole nitrogen source. Since a relatively low nitrate concentration was required the calcium nitrate present in Hoagland medium was replaced by calcium chloride (for medium composition and preparation see Supplementary File S11). Thus, the medium contained a relatively high but constant chloride concentration. Constant aeration of the medium was provided by air stones connected to an air pump. Plants were cultivated at 21 °C with a 16 h light/8 h dark cycle and a light intensity of 100 μmol·s^{-1}·m^{-2}. After 29 days in the initial medium plants were switched to medium containing [^{14}N]-nitrate. Roots were rinsed with deionized water before transfer to the other medium. Sampling of leaf discs was performed over a 19-day period.

Plants used for preparation of nitrate-free leaf extracts used for investigating the matrix effect (see point 4.4.6.) were cultivated on low nutrient soil SP ED63 P (Patzer GmbH and Co. KG, Sinntal-Altengronau, Germany; initial nitrate content: 555 mg/kg dry weight) for 12 weeks. The plants showed nitrogen

deficiency symptoms three weeks prior to harvest and absence of nitrate in the leaf extracts was confirmed by ion-pair chromatography and by GC–MS.

4.3. Sample Preparation and GC–MS

Leaf discs with 8 mm diameter (approximately 10 mg) were cut out using a hollow punch, placed into 2 mL safe lock tubes and stored at –20 °C until analysis. Distilled water (150 µL) was added and the tube incubated in a Thermomix shaker (Eppendorf, Hamburg, Germany) set to 1400 rpm and 95 °C for 20 min. After centrifugation at 10,000 rpm for 2 min the nitrate concentration was quantified by ion-pair chromatography (see Section 4.7). and the remaining extract diluted to a final nitrate concentration of 0.2–0.4 mM if required. A 2 mL safe lock tube was charged with 100 µL extract, 600 µL 80% sulfuric acid, and 10 µL mesitylene. The tubes were placed in a Thermomix shaker set to 1400 rpm at room temperature for 20 min. Water (500 µL) containing 0.01% indigo carmine and 190 µL heptane were added and the tubes shaken vigorously prior centrifugation at 10,000 rpm for 30 s. Approximately 150 µL of the supernatant was transferred into a 1.5 mL reaction tube containing approximately 5 mg sodium carbonate and mixed vigorously. After centrifugation at 10,000 rpm for 30 s, 80 µL of the clear supernatant was transferred into an autosampler tube.

A Varian 431-GC gas chromatograph equipped with a CP-8400 autosampler and connected to a 210-MS mass spectrometer (Palo Alto, CA, USA) was used. For analysis, a VF-5ms 30 m × 0.25 mm × 0.25 µm capillary column was used. Helium was used as carrier gas at a flow rate of 1 mL/min and a split ration of 10. The injector was set to 230 °C. Injection (1 µL sample) was performed at a split ratio of 1. The temperature program started with an isothermal step at 120 °C for 1 min. Then the temperature was raised linearly within 4 min to 200 °C at a rate of 20 °C/min. Finally, the temperature was raised within 1 min to 260 °C at a rate of 60 °C prior returning to the initial conditions. The transfer line was operated at 200 °C, the ion trap at 160 °C, and the manifold at 40 °C. MS spectra were recorded from 3.6 to 4.8 min and from m/z 50 to 200. For establishing the calibration curve the sum of the intensities of the ions with m/z 149 and 150 was divided by the sum of the ions with m/z 148 + 149 + 150 and plotted on the y-axis while mol% of [15N]-nitrate was plotted on the x-axis. A detailed step-by-step protocol is included in Appendix A.

4.4. Method Development

4.4.1. Initial Testing of Different Derivatization Methods

Derivatization with mesitylene was performed according to Dunphy et al. [90] except that no internal standard was added. Derivatization with 1,3,5-trimetrhoxybenzen was performed as described by Gutzki et al. [92] except that the reaction product was extracted with toluene rather than benzene. For derivatization with 2,3,4,5,6-pentafluorobenzyl bromide the protocols of Tsikas et al. [94] and of Kage et al. [93] were applied. Derivatization with benzene was adapted from [89]. In brief, 100 µL of sample was mixed with 600 µL of 85% sulfuric acid and 200 µL of benzene in 2 mL safe lock tubes. The tubes were shaken at room temperature in an Eppendorf Thermomixer (Hamburg, Germany) set to 1400 rpm for 15 min. The upper layer was transferred to a tube containing approximately 5 mg sodium carbonate, shaken vigorously and centrifuged at 10,000 × g for 30 s. The supernatant was directly analyzed. The reaction product with benzene was analyzed by GC–MS as stated above except that the temperature program was modified: isothermal at 100 °C for 1 min, then a liner increase to 180 °C within 4 min, and finally a linear increase to 260 °C within 2 min prior returning to the initial conditions. The other derivatization products were analyzed using the settings mentioned in Section 4.4.2.

4.4.2. Optimization of Reaction Time and Sulfuric Acid Concentration

Sample (100 µL; 1 mM [14N]-potassium nitrate) was mixed with 600 µL sulfuric acid of the indicated concentration and 300 µL mesitylene containing 0.5 mM 2,4-dinitrotoluene as the internal

standard. The mixture was derivatized and processed as stated above except that a reaction time of 5, 10, or 20 min was used. The clear supernatant was analyzed by GC–MS as described above except that the following GC settings were used: injector temperature 250 °C; thermal program: isothermal at 120 °C for 1 min, then a linear increase to 230 °C within 5.5 min, and finally a linear increase to 290 °C within 1.5 min prior returning to the initial conditions. MS spectra were recorded from 3.6 to 4.8 min and from *m/z* 50 to 200.

4.4.3. Optimization of Mesitylene Amount and Sulfuric Acid Concentration

Sample (100 µL; 0.5 mM [^{14}N]-potassium nitrate) was mixed with 600 µL of 80% or 85% sulfuric acid and 5, 10, 20, 50, 100, or 150 µL mesitylene was added. The mixture was shaken at 1400 rpm at room temperature for 20 min. The reaction was stopped by addition of 500 µL of water containing 0.01% indigo carmine. Subsequently, 50 µL of 0.5 mM 2,4-dinitrotoluene dissolved in mesitylene was added as the internal standard and heptane was added to complete the organic phase to 200 µL. The supernatants were processed and analyzed as described in Section 4.4.2.

4.4.4. Test for Linearity

Potassium nitrate solutions (100 µL of [^{14}N]-potassium nitrate or 100 µL of [^{15}N]-potassium nitrate) of different concentrations (0, 0.005, 0.01, 0.02, 0.05, 0.1, 0.2, 0.5, and 1 mM) were analyzed as described in Section 4.4.3.

4.4.5. Stability of the Reaction Products

A sample was derivatized with 20 µL of mesitylene as described in Section 4.4.3. The derivatized solution was measured on five consecutive days with five replicates on each day. The derivatized sample was stored at room temperature.

4.4.6. Matrix Effect

Nitrate-free plant extracts obtained from *C. crepidioides* leaves were spiked with a mixture of [^{14}N] and [^{15}N]-potassium nitrate to a total concentration of 0.4 mM nitrate. The phenolic contents were assayed as described in Section 4.8. [^{15}N] and [^{14}N]-nitrate were measured as described in Section 4.4.3.

4.5. Method Validation

A sample containing 0.4 mM [^{14}N]-nitrate was measured 9 times and the average and SD were calculated. The LOD and LOQ were calculated by dividing the 3-fold and 10-fold SD by the slope of the calibration curve, respectively.

For testing the repeatability, samples with a medium and high content of phenolics were spiked with a mixture of [^{14}N] and [^{15}N]-potassium nitrate to a total concentration of 0.4 mM nitrate. The samples were analyzed on five consecutive days with five replicates on each day. Every day a calibration curve (see Appendix A for details) was established.

4.6. Quantification of Nitrate in Leaf Extracts by Ion-Pair Chromatography

Quantification of nitrate by ion-pair chromatography was adapted from Chou et al. [60]. A Shimadzu 10A high performance liquid chromatography system (Shimadzu, Kyoto, Japan) was used. The HPLC system consisted of a SCL-10A system controller, a FCV-10AL valve for eluent selection, a LC-10AT pump equipped with DGU-14A inline degasser, a SIL-10A autosampler, a CTO-10ASvp column oven set to 25 °C, a Nucleodur 100-5 C18ec 125 × 4.6 mm HPLC column (Machery-Nagel, Düren, Germany), and a SPD-10A UV detector, which was operated at 213 nm. The eluent consisted of 10 mM 1-octylamine set with phosphoric acid to pH 7.0 in 20% ACN (acetonitrile). For elution, a flow rate of 1 mL/ min was set and the injection volume was 25 µL. Samples were diluted with eluent 1:10 prior to injection. Standards were dissolved in eluent and contained nitrate in the range

of 0–10 mg/L. Chromatograms were evaluated with the Clarity software package (version 5.0.4.158, DataApex, Prague, Czech Republic).

4.7. Analysis of Cations and Anions in Hydroponic Media by Ion Chromatography

For analysis of cations the samples were diluted 1:50 by transferring 1 mL of sample into a 50 mL volumetric flask and adding deionized water to the mark. An aliquot was transferred into a polypropylene autosampler vial and 100 μL was injected into the ion chromatograph. The ion chromatograph consisted of a LC-10ADvp pump, a FCV-10ALvp valve for eluent selection, a SIL-10A autosampler, a CTO-10ASvp column (Shimadzu), a Nucleodur 100-5 C18ec 4 × 3 mm pre-column, an IC-Pak Cation M/D 3.9 × 150 mm column (Waters, Milford, MA, USA), and a 430 conductivity detector (Waters). Chromatograms were evaluated with the Clarity software package. The column oven was maintained at 25 °C. The eluent consisted of 3 mM nitric acid and 0.1 mM EDTA (ethylenediaminetetraacetic acid) and was delivered at a flow rate of 1 mL/min. Standards contained sodium (0–0.05 mM), ammonium (0–0.05 mM), potassium (0–0.25 mM), magnesium (0–0.25 mM), and calcium (0–0.5 mM).

Anions were analyzed by diluting the samples 1:5 by transferring 1 mL of sample into a 5 mL volumetric flask and adding deionized water to the mark. An aliquot was transferred into a polypropylene autosampler vial and 100 μL was injected into the ion chromatograph described above except that an IC-PAK Anion HC 150 × 4.6 mm column (Waters) and a sodium gluconate/borate buffer (sodium gluconate 320 mg/L, boric acid 360 mg/L, disodium tetraborate 264 mg/L, glycerol 4 g/L, acetonitrile 12%, and 1-butanol 2%) delivered at a flow rate of 1.6 mL/min were used. The standards contained chloride (0–6.42 mM), nitrate (0–1.7 mM), phosphate (0–0.4 mM), and sulfate (0–1.81 mM).

4.8. Determination of Total Phenolics in Leaf Extracts

The method was adapted from Veliogli et al. [110]. In brief, suitable volumes of sample or standard (0–50 μL of 0.1 mM ferulic acid) were transferred into 1 mL plastic cuvettes and water was added to a total volume of 700 μL. Subsequently, 50 μL of Folin–Ciocalteu reagent was added. After mixing and incubating at room temperature for 5 min, 250 μL of 2 M sodium carbonate was added and mixed well. The absorbance was measured at 725 nm after incubation for 1 h at room temperature. The results were expressed in mM ferulic acid equivalents.

Appendix A

Step-by-Step Protocol for Determination of the [^{15}N]-Nitrate/[^{14}N]-Nitrate Ration in Leaves

Appendix A.1.1. Reagents

- [^{14}N]-Nitrate stock, 1 mM (transfer 101.1 mg [^{14}N]-potassium nitrate into a 1000 mL volumetric flask, dissolve in distilled water and add distilled water to the mark. The solution is stable for one week at 4 °C or for at least 2 years at −20 °C).
- [^{15}N]-Nitrate stock, 1 mM (transfer 102.1 mg [^{15}N]-potassium nitrate into a 1000 mL volumetric flask, dissolve in distilled water and add distilled water to the mark. The solution is stable for one week at 4 °C or for at least 2 years at −20 °C).
- Sulfuric acid, 80% (*w/w*) (place 54 mL distilled water in a 250 mL flask and cool with ice; add in total 146 mL sulfuric acid, 96% (*w/w*) under cooling with ice slowly and in small aliquots. The solution can be stored at room temperature infinitely).
- Mesitylene
- Water containing 0.01% indigo carmine (dissolve approximately 10 mg indigo carmine in 100 mL water and add 100 μL 80% sulfuric acid; the solution can be kept at room temperature for at least one month).
- Heptane
- Eluent for ion-pair chromatography: 10 mM 1-octylamine phosphate pH 7.0 in 20% (*v/v*) ACN (transfer 1.29 g 1-octylamine and 156.4 g ACN (note: this corresponds to 200 mL ACN) into a 1000 mL beaker and add approximately 700 mL distilled water. Set the pH with 4 M phosphoric acid to 7.0. Transfer into a 1000 mL volumetric flask and add distilled water to the mark. Filter through a 0.22 or 0.45 μm nylon membrane filter. The eluent can be kept at room temperature for at least 1 year).

Appendix A.1.2. Preparation of Standards

1. Mix the solutions indicated in Table A1 in 5 mL volumetric flasks:

Table A1. Preparation of standards.

No.	[^{15}N]-Nitrate 1 mM μL	[^{14}N]-Nitrate 1 mM μL	[^{15}N]-Nitrate [1,2] mol%
St1	0	1000	0.366
St2	10	990	1.352
St3	20	980	2.339
St4	50	950	5.298
St5	100	900	10.299
St6	200	800	20.093
St7	400	600	39.820
St8	600	400	59.546
St9	800	200	79.273
St10	1000	0	99.000

[1] The total nitrate concentration is 0.2 mM; [2] Calculated for 99.634 mol% isotope purity, the natural frequency of ^{14}N, for [^{14}N]-nitrate and 99 mol% isotope purity of [^{15}N]-nitrate. Standards prepared from stocks with other purities can be calculated using Supplementary File S12.

2. Add water to the mark. The standards can be kept at −20 °C for at least two years.

Appendix A.1.3. Extraction

1. Punch out leaf discs of 8 mm diameter using a hollow punch. These discs weigh approximately 10 mg.

2. Transfer the leaf discs into 2 mL safe lock tubes and store at –20 °C until analysis.
3. Add 150 µL distilled water, incubate in a shaker set to 1400 rpm and 95 °C for 20 min.
4. Centrifuge at 10,000 rpm for 2 min.
5. Transfer the clear supernatant into a new tube and measure the nitrate content by ion-pair chromatography or proceed immediately to derivatization. The extract can be stored at −20 °C for several days.

Appendix A.1.4. Derivatization and Analysis

1. Transfer 100 µL of leaf extract or standard (see Table A1) into a 2 mL safe-lock tube. Note: if the nitrate concentration was determined, dilute the extract to a final nitrate concentration of approximately 0.2 mM prior transferring 100 µL into the 2 mL safe lock tube.
2. Add 10 µL mesitylene.
3. Add 600 µL 80% sulfuric acid.
4. Incubate the tubes at room temperature in a shaker set to 1400 rpm for 20 min.
5. Add 500 µL water containing 0.01% indigo carmine and 190 µL heptane and mix again for 1 min.
6. Centrifuge at 10,000 g for 30 s.
7. Transfer 150 µL of the upper, colorless organic phase into a 1.5 mL tube containing approximately 5 mg sodium carbonate. Avoid transferring any of the aqueous phase. Note: indigo carmine stains the lower aqueous phase intensively blue, which helps with recognizing the phases.
8. Shake the tubes vigorously for a few seconds.
9. Centrifuge at 10,000 g for 30 s.
10. Transfer 80 µL of the clear supernatant into an autosampler vial.
11. Analyze the samples by GC–MS using a VF-5ms 30 m × 0.25 mm × 0.25 µm capillary column and helium as carrier gas at a flow rate of 1 mL/min and a split ratio of 1:10. The injector is set to 230 °C. Injection (1 µL sample) is performed with a split of 1. The temperature program is set according to Table A2. The transfer line is operated at 200 °C, the ion trap at 160 °C, and the manifold at 40 °C. MS spectra are recorded from 3.6 to 4.8 min and from m/z 70 to 170. Alternatively, SIM (selected ion monitoring) for m/z 148, 149, and 150 can be applied. Typical chromatograms and MS spectra are shown in Figures 1 and 5, respectively. For evaluation the intensities of the ions of m/z 148, 149, and 150 are used; the sum of the intensities of m/z 149 + 150 is divided by the sum of the intensities of m/z 148 + 149 + 150. These values are plotted against the mol% of [^{15}N]-nitrate (see Table A1). A linear curve is obtained.

Table A2. Colum oven program for GC–MS.

Time min	Temperature °C	Heating Rate °C/min
0	120	0
1	120	20
5	200	60
6	260	—

Appendix A.1.5. Optional: Determination of the Nitrate Concentration by Ion-Pair Chromatography

1. Mix exactly 20 µL extract with 180 µL eluent and centrifuge at 10,000 rpm for 5 min.
2. Prepare standards according to Table A3.

Table A3. Preparation of standards for nitrate quantification.

No.	Final Nitrate Concentration in mM	Nitrate Stock 1 mM [1] µL
St1	0	0
St2	0.001	10
St3	0.002	20
St4	0.005	50
St5	0.01	100
St6	0.02	200
St7	0.05	500
St8	0.1	1000

[1] The stock solution must be transferred into a 10 mL volumetric flask and eluent for ion-pair chromatography added to the mark. Usually 1 mM [^{14}N]-nitrate is used but 1 mM [^{15}N]-nitrate is also suitable.

3. Transfer 150 µL of the clear supernatant into an autosampler vial and analyze by ion-pair chromatography using an HPLC system with the following settings:

- Column: Nucleodur 100-5 C18ec 125 × 4.6 mm
- Precolumn: Nucleodur 100-5 C18ec 125 × 4.6 mm
- Injection volume: 25 µL
- Column oven: 25 °C
- Detector: UV, 213 nm
- Eluent: eluent for ion-pair chromatography: 10 mM 1-octylamine phosphate pH 7.0 in 20% (*v/v*) ACN
- Flow rate: 1 mL/min
- Isocratic elution
- Analysis time: 5 min

References

1. Mansour, M. Nitrogen Containing Compounds and Adaptation of Plants to Salinity Stress. *Biol. Plant.* **2000**, *43*, 491–500. [CrossRef]
2. Kim, N.; Estrada, O.; Chavez, B.; Stewart, C.; D'Auria, J.C. Tropane and Granatane Alkaloid Biosynthesis: A Systematic Analysis. *Molecules* **2016**, *21*, 1510. [CrossRef] [PubMed]
3. Kishimoto, S.; Sato, M.; Tsunematsu, Y.; Watanabe, K. Evaluation of Biosynthetic Pathway and Engineered Biosynthesis of Alkaloids. *Molecules* **2016**, *21*, 1078. [CrossRef] [PubMed]
4. Schramm, S.; Kohler, N.; Rozhon, W. Pyrrolizidine Alkaloids: Biosynthesis, Biological Activities and Occurrence in Crop Plants. *Molecules* **2019**, *24*, 498. [CrossRef] [PubMed]
5. Ziegler, J.; Facchini, P.J. Alkaloid biosynthesis: Metabolism and trafficking. *Annu. Rev. Plant Biol.* **2008**, *59*, 735–769. [CrossRef] [PubMed]
6. Ishida, M.; Hara, M.; Fukino, N.; Kakizaki, T.; Morimitsu, Y. Glucosinolate metabolism, functionality and breeding for the improvement of Brassicaceae vegetables. *Breed. Sci.* **2014**, *64*, 48–59. [CrossRef]
7. Vig, A.P.; Rampal, G.; Thind, T.S.; Arora, S. Bio-protective effects of glucosinolates—A review. *LWT-Food Sci. Technol.* **2009**, *42*, 1561–1572. [CrossRef]
8. Niculaes, C.; Abramov, A.; Hannemann, L.; Frey, M. Plant Protection by Benzoxazinoids—Recent Insights into Biosynthesis and Function. *Agronomy* **2018**, *8*, 143. [CrossRef]
9. Pedras, M.S.; Yaya, E.E. Phytoalexins from Brassicaceae: News from the front. *Phytochemistry* **2010**, *71*, 1191–1197. [CrossRef]
10. Walker, R.L.; Burns, I.G.; Moorby, J. Responses of plant growth rate to nitrogen supply: A comparison of relative addition and N interruption treatments. *J. Exp. Bot.* **2001**, *52*, 309–317. [CrossRef]
11. Ekandjo, L.K.; Ruppel, S. The impact of mineral nitrogen fertilization on the occurrence of native diazotrophic bacteria in kohlrabi (*Brassica oleracea*) shoots and roots. *J. Agric. Sci.* **2015**, *7*, 1. [CrossRef]

12. Ishii, S.; Ikeda, S.; Minamisawa, K.; Senoo, K. Nitrogen cycling in rice paddy environments: Past achievements and future challenges. *Microbes Environ.* **2011**, *26*, 282–292. [CrossRef]

13. Jackson, L.E.; Schimel, J.P.; Firestone, M.K. Short-term partitioning of ammonium and nitrate between plants and microbes in an annual grassland. *Soil Biol. Biochem.* **1989**, *21*, 409–415. [CrossRef]

14. Kiyomiya, S.; Nakanishi, H.; Uchida, H.; Tsuji, A.; Nishiyama, S.; Futatsubashi, M.; Tsukada, H.; Ishioka, N.S.; Watanabe, S.; Ito, T.; et al. Real time visualization of ^{13}N-translocation in rice under different environmental conditions using positron emitting tracer imaging system. *Plant Physiol.* **2001**, *125*, 1743–1753. [CrossRef]

15. Schjoerring, J.K.; Husted, S.; Mack, G.; Mattsson, M. The regulation of ammonium translocation in plants. *J. Exp. Bot.* **2002**, *53*, 883–890. [CrossRef]

16. Yoneyama, T.; Suzuki, A. Exploration of nitrate-to-glutamate assimilation in non-photosynthetic roots of higher plants by studies of (15)N-tracing, enzymes involved, reductant supply, and nitrate signaling: A review and synthesis. *Plant Physiol. Biochem.* **2019**, *136*, 245–254. [CrossRef]

17. Miflin, B.J.; Lea, P.J. Amino acid metabolism. *Ann. Rev. Plant Physiol.* **1977**, *28*, 299–329. [CrossRef]

18. Vines, H.M.; Wedding, R.T. Some effects of ammonia on plant metabolism and a possible mechanism for ammonia toxicity. *Plant Physiol.* **1960**, *35*, 820–825. [CrossRef]

19. van der Eerden, L.J.M. Toxicity of ammonia to plants. *Agric. Environ.* **1982**, *7*, 223–235. [CrossRef]

20. Britto, D.T.; Kronzucker, H.J. NH_4^+ toxicity in higher plants: A critical review. *J. Plant Physiol.* **2002**, *159*, 567–584. [CrossRef]

21. Oke, O.L. Nitrite toxicity to plants. *Nature* **1966**, *212*, 528. [CrossRef]

22. Krouk, G. Hormones and nitrate: A two-way connection. *Plant Mol. Biol.* **2016**, *91*, 599–606. [CrossRef] [PubMed]

23. Krapp, A. Plant nitrogen assimilation and its regulation: A complex puzzle with missing pieces. *Curr. Opin. Plant Biol.* **2015**, *25*, 115–122. [CrossRef] [PubMed]

24. Wang, M.; Shen, Q.; Xu, G.; Guo, S. New insight into the strategy for nitrogen metabolism in plant cells. *Int. Rev. Cell Mol. Biol.* **2014**, *310*, 1–37. [CrossRef] [PubMed]

25. Dreccer, M.F.; Schapendonk, A.H.C.M.; Slafer, G.A.; Rabbinge, R. Comparative response of wheat and oilseed rape to nitrogen supply:absorption and utilisation efficiency of radiation and nitrogen during thereproductive stages determining yield. *Plant Soil* **2000**, *220*, 189–205. [CrossRef]

26. Fischer, R.A. Irrigated spring wheat and timing and amount of nitrogen fertilizer. II. Physiology of grain yield response. *Field Crops Res.* **1993**, *33*, 57–80. [CrossRef]

27. Ma, B.L.; Dwyer, L.M.; Gregorich, E.G. Soil nitrogen amendment effects on nitrogen uptake and grain yield of maize. *Agron. J.* **1998**, *91*, 650–656. [CrossRef]

28. Coque, M.; Gallais, A. Genomic regions involved in response to grain yield selection at high and low nitrogen fertilization in maize. *Theor. Appl. Genet.* **2006**, *112*, 1205–1220. [CrossRef]

29. Belay, A.; Claassens, A.; Wehner, F. Effect of direct nitrogen and potassium and residual phosphorus fertilizers on soil chemical properties, microbial components and maize yield under long-term crop rotation. *Biol. Fertil. Soils* **2002**, *35*, 420–427. [CrossRef]

30. Collins, M.; Brinkman, M.A.; Salman, A.A. Forage yield and quality of oat cultivars with increasing rates of nitrogen fertilization. *Agron. J.* **1990**, *82*, 724–728. [CrossRef]

31. Hansson, A.C.; Pettersson, R.; Paustian, K. Shoot and root production and nitrogen uptake in barley, with and without nitrogen fertilization. *J. Agron. Crop Sci.* **1987**, *158*, 163–171. [CrossRef]

32. Oscarsson, M.; Andersson, R.; Åman, P.; Olofsson, S.; Jonsson, A. Effects of cultivar, nitrogen fertilization rate and environment on yield and grain quality of barley. *J. Sci. Food Agric.* **1998**, *78*, 359–366. [CrossRef]

33. Steer, B.T.; Hocking, P.J.; Kortt, A.A.; Roxburgh, C.M. Nitrogen nutrition of sunflower (*Helianthus annuus* L.): Yield components, the timing of their establishment and seed characteristics in response to nitrogen supply. *Field Crops Res.* **1984**, *9*, 219–236. [CrossRef]

34. Bélanger, G.; Walsh, J.R.; Richards, J.E.; Milburn, P.H.; Ziadi, N. Nitrogen fertilization and irrigation affects tuber characteristics of two potato cultivars. *Am. J. Potato Res.* **2002**. [CrossRef]

35. Westermann, D.T.; Tindall, T.A.; James, D.W.; Hurst, R.L. Nitrogen and potassium fertilization of potatoes: Yield and specific gravity. *Am. Potato J.* **1994**, *71*, 417–431. [CrossRef]

36. Malnou, C.S.; Jaggard, K.W.; Sparkes, D.L. Nitrogen fertilizer and the efficiency of the sugar beet crop in late summer. *Eur. J. Agron.* **2008**, *28*, 47–56. [CrossRef]

37. Elia, A.; Santamaria, P.; Serio, F. Nitrogen nutrition, yield and quality of spinach. *J. Sci. Food Agric.* **1998**, *76*, 341–346. [CrossRef]

38. Aronsson, P.; Rosenqvist, H.; Dimitriou, I. Impact of nitrogen fertilization to short-rotation willow coppice plantations grown in sweden on yield and economy. *Bioenergy Res.* **2014**, *7*, 993–1001. [CrossRef]

39. Ercoli, L.; Mariotti, M.; Masoni, A.; Bonaria, E. Effect of irrigation and nitrogen fertilization on biomass yield and efficiency of energy use in crop production of *Miscanthus*. *Field Crops Res.* **1999**, *63*, 3–11. [CrossRef]

40. Vargas, M.; Mendes, I.; Hungria, M. Response of field-grown bean (*Phaseolus vulgaris* L.) to *Rhizobium* inoculation and nitrogen fertilization in two Cerrados soils. *Biol. Fertil. Soils* **2000**, *32*, 228. [CrossRef]

41. Brkić, S.; Milaković, Z.; Kristek, A.; Antunović, M. Pea yield and its quality depending on inoculation, nitrogen and molybdenum fertilization. *Plant Soil Environ.* **2004**, *50*, 39–45. [CrossRef]

42. Ahmed, M.; Rauf, M.; Mukhtar, Z.; Saeed, N.A. Excessive use of nitrogenous fertilizers: An unawareness causing serious threats to environment and human health. *Environ. Sci. Pollut. Res. Int.* **2017**, *24*, 26983–26987. [CrossRef]

43. Penna, N.; Capellacci, S.; Ricci, F. The influence of the Po River discharge on phytoplankton bloom dynamics along the coastline of Pesaro (Italy) in the Adriatic Sea. *Mar. Pollut. Bull.* **2004**, *48*, 321–326. [CrossRef]

44. Chen, B.M.; Wang, Z.H.; Li, S.X.; Wang, G.X.; Song, H.X.; Wang, X.N. Effects of nitrate supply on plant growth, nitrate accumulation, metabolic nitrate concentration and nitrate reductase activity in three leafy vegetables. *Plant Sci.* **2004**, *167*, 635–643. [CrossRef]

45. Anjana, S.U.; Iqbal, M. Nitrate accumulation in plants, factors affecting the process, and human health implications. A review. *Agron. Sustain. Dev.* **2007**, *27*, 45–57. [CrossRef]

46. Nunez de Gonzalez, M.T.; Osburn, W.N.; Hardin, M.D.; Longnecker, M.; Garg, H.K.; Bryan, N.S.; Keeton, J.T. A survey of nitrate and nitrite concentrations in conventional and organic-labeled raw vegetables at retail. *J. Food Sci.* **2015**, *80*, C942–C949. [CrossRef]

47. Aires, A.; Carvalho, R.; Rosa, E.A.; Saavedra, M.J. Effects of agriculture production systems on nitrate and nitrite accumulation on baby-leaf salads. *Food Sci. Nutr.* **2013**, *1*, 3–7. [CrossRef]

48. Espejo-Herrera, N.; Gracia-Lavedan, E.; Boldo, E.; Aragones, N.; Perez-Gomez, B.; Pollan, M.; Molina, A.J.; Fernandez, T.; Martin, V.; La Vecchia, C.; et al. Colorectal cancer risk and nitrate exposure through drinking water and diet. *Int. J. Cancer* **2016**, *139*, 334–346. [CrossRef]

49. Taneja, P.; Labhasetwar, P.; Nagarnaik, P.; Ensink, J.H.J. The risk of cancer as a result of elevated levels of nitrate in drinking water and vegetables in Central India. *J. Water Health* **2017**, *15*, 602–614. [CrossRef]

50. Taneja, P.; Labhasetwar, P.; Nagarnaik, P. Nitrate in drinking water and vegetables: Intake and risk assessment in rural and urban areas of Nagpur and Bhandara districts of India. *Environ. Sci. Pollut. Res. Int.* **2019**, *26*, 2026–2037. [CrossRef]

51. Hord, N.G.; Tang, Y.; Bryan, N.S. Food sources of nitrates and nitrites: The physiologic context for potential health benefits. *Am. J. Clin. Nutr.* **2009**, *90*. [CrossRef]

52. Gopinath, B.; Liew, G.; Kifley, A.; Lewis, J.R.; Bondonno, C.; Joachim, N.; Hodgson, J.M.; Mitchell, P. Association of Dietary Nitrate Intake with the 15-Year Incidence of Age-Related Macular Degeneration. *J. Acad. Nutr. Diet.* **2018**, *118*, 2311–2314. [CrossRef]

53. Jackson, J.K.; Patterson, A.J.; MacDonald-Wicks, L.K.; Forder, P.M.; Blekkenhorst, L.C.; Bondonno, C.P.; Hodgson, J.M.; Ward, N.C.; Holder, C.; Oldmeadow, C.; et al. Vegetable Nitrate Intakes Are Associated with Reduced Self-Reported Cardiovascular-Related Complications within a Representative Sample of Middle-Aged Australian Women, Prospectively Followed up for 15 Years. *Nutrients* **2019**, *11*, 240. [CrossRef]

54. Liu, A.H.; Bondonno, C.P.; Russell, J.; Flood, V.M.; Lewis, J.R.; Croft, K.D.; Woodman, R.J.; Lim, W.H.; Kifley, A.; Wong, G.; et al. Relationship of dietary nitrate intake from vegetables with cardiovascular disease mortality: A prospective study in a cohort of older Australians. *Eur. J. Nutr.* **2018**. [CrossRef]

55. Gorenjak, A.H.; Cencič, A. Nitrate in vegetables and their impact on human health. A review. *Acta Aliment.* **2013**, *42*, 58–72. [CrossRef]

56. Bray, R.H. Nitrates tests for soils and plant tissues. *Soil Sci.* **1945**, *60*, 219–222. [CrossRef]

57. Nelson, J.L.; Kurtz, L.T.; Bray, R.H. Rapid determination of nitrates and nitrites. *Anal. Chem.* **1954**, *26*, 1081–1082. [CrossRef]

58. Milham, P.J.; Awad, A.S.; Paull, R.E.; Bull, J.H. Analysis of plants, soils and waters for nitrate by using an ion-selective electrode. *Analyst* **1970**, *95*, 751–757. [CrossRef]

59.　Bosch Bosch, N.; García Mata, M.; Peñuela, M.J.; Ruiz Galán, T.; López Ruiz, B. Determination of nitrite levels in refrigerated and frozen spinach by ion chromatography. *J. Chromatogr. A* **1995**, *706*, 221–228. [CrossRef]

60.　Chou, S.S.; Chung, J.C.; Hwang, D.F. A high performance liquid chromatography method for determining nitrate and nitrite levels in vegetables. *J. Food Drug Anal.* **2003**, *11*, 233–238.

61.　Tesch, J.W.; Rehg, W.R.; Sievers, R.E. Microdetermination of nitrates and nitrites in saliva, blood, water, and suspended particulates in air by gas chromatography. *J. Chromatogr. A* **1976**, *126*, 743–755. [CrossRef]

62.　Jimidar, M.; Hartmann, C.; Cousement, N.; Massart, D.L. Determination of nitrate and nitrite in vegetables by capillary electrophoresis with indirect detection. *J. Chromatogr. A* **1995**, *706*, 479–492. [CrossRef]

63.　Atilio, B.; Causin, H.F. The central role of amino acids on nitrogen utilization and plant growth. *J. Plant Physiol.* **1996**, *149*, 358–362. [CrossRef]

64.　Atanasova, E. Effect of nitrogen sources on the nitrogenous forms and accumulation of amino acid in head cabbage. *Plant Soil Environ.* **2008**, *54*, 66–71. [CrossRef]

65.　van den Driessche, R.; Rieche, K. Prediction of mineral nutrient status of trees by foliar analysis. *Bot. Rev.* **1974**, *40*, 347–394. [CrossRef]

66.　Agius, C.; von Tucher, S.; Poppenberger, B.; Rozhon, W. Quantification of Glutamate and Aspartate by Ultra-High Performance Liquid Chromatography. *Molecules* **2018**, *23*, 1389. [CrossRef]

67.　Ammann, M.; Stalder, M.; Suter, M.; Brunold, C.; Baltensperger, U.; Jost, D.T.; Türler, A.; Gäggeler, H.W. Tracing uptake and assimilation of NO_2 in spruce needles with ^{13}N. *J. Exp. Bot.* **1995**, *46*, 1685–1691. [CrossRef]

68.　Hanson, A.D.; Tully, R.E. Amino acids translocated from turgid and water-stressed barley leaves: II. studies with ^{13}N and ^{14}C. *Plant Physiol.* **1979**, *64*, 467–471. [CrossRef]

69.　Schubert, K.R.; Coker, G.T. Ammonia assimilation in *Alnus glutinosa* and *Glycine max*: Short-term studies using [^{13}N]ammonium. *Plant Physiol.* **1981**, *67*, 662–665. [CrossRef]

70.　Azuelos, G.; Kitching, J.E.; Ramavataram, K. Half-lives and branching ratios of some T=1/2 nuclei. *Phys. Rev. C* **1977**, *15*, 1847–1851. [CrossRef]

71.　Junk, G.; Svec, H.J. The absolute abundance of the nitrogen isotopes in the atmosphere and compressed gas from various sources. *Geochim. Cosmochim. Acta* **1958**, *14*, 234–243. [CrossRef]

72.　Duque, F.F.; Neves, M.C.P.; Franco, A.A.; Victoria, R.L.; Boddey, R.M. The response of field grown *Phaseolus vulgaris* to *Rhizobium* inoculation and the quantification of N_2 fixation using ^{15}N. *Plant Soil* **1985**, *88*, 333–343. [CrossRef]

73.　Avice, J.C.; Ourry, A.; Lemaire, G.; Boucaud, J. Nitrogen and carbon flows estimated by ^{15}N and ^{13}C pulse-chase labeling during regrowth of alfalfa. *Plant Physiol.* **1996**, *112*, 281–290. [CrossRef] [PubMed]

74.　Lewis, O.A.M.; Chadwick, S. ^{15}N investigation into nitrogen assimilation in hydroponically-grown barley (*Hordeum vulgare* L. cv. Clipper) in response to nitrate, ammonium and mixed nitrate and ammonium nutrition. *New Phytol.* **1983**, *95*, 635–646. [CrossRef]

75.　Soares, M.I.M.; Lewis, O.A.M. An investigation into nitrogen assimilation and distribution in fruiting plants of barley (*Hordeum vulgare* L. cv. Clipper) in response to nitrate, ammonium and mixed nitrate and ammonium nutrition. *New Phytol.* **1986**, *104*, 385–393. [CrossRef]

76.　Schiltz, S.; Munier-Jolain, N.; Jeudy, C.; Burstin, J.; Salon, C. Dynamics of exogenous nitrogen partitioning and nitrogen remobilization from vegetative organs in pea revealed by ^{15}N in vivo labeling throughout seed filling. *Plant Physiol.* **2005**, *137*, 1463–1473. [CrossRef] [PubMed]

77.　Thorpe, T.A.; Bagh, K.; Cutler, A.J.; Dunstan, D.I.; McIntyre, D.D.; Vogel, H.J. A ^{14}N and ^{15}N Nuclear Magnetic Resonance Study of Nitrogen Metabolism in Shoot-Forming Cultures of White Spruce (*Picea glauca*) Buds. *Plant Physiol.* **1989**, *91*, 193–202. [CrossRef] [PubMed]

78.　Kikuchi, J.; Shinozaki, K.; Hirayama, T. Stable isotope labeling of Arabidopsis thaliana for an NMR-based metabolomics approach. *Plant Cell Physiol.* **2004**, *45*, 1099–1104. [CrossRef]

79.　Gartia, J.; Barnwal, R.P.; Anangi, R.; Giri, A.R.; King, G.; Chary, K.V.R. ^{1}H, ^{13}C and ^{15}N NMR assignments of two plant protease inhibitors (IRD7 and IRD12) from the plant *Capsicum annuum*. *Biomol. NMR Assign.* **2018**. [CrossRef]

80.　Gentile, N.; Rossi, M.J.; Delemont, O.; Siegwolf, R.T. delta^{15}N measurement of organic and inorganic substances by EA-IRMS: A speciation-dependent procedure. *Anal. Bioanal. Chem.* **2013**, *405*, 159–176. [CrossRef]

81. Trandel, M.A.; Vigardt, A.; Walters, S.A.; Lefticariu, M.; Kinsel, M. Nitrogen Isotope Composition, Nitrogen Amount, and Fruit Yield of Tomato Plants Affected by the Soil-Fertilizer Types. *ACS Omega* **2018**, *3*, 6419–6426. [CrossRef]

82. Evans, R.D. Physiological mechanisms influencing plant nitrogen isotope composition. *Trends Plant Sci.* **2001**, *6*, 121–126. [CrossRef]

83. Ma, Z.; Barich, D.H.; Solum, M.S.; Pugmire, R.J. Solid-state 15N NMR studies of tobacco leaves. *J. Agric. Food Chem.* **2004**, *52*, 215–221. [CrossRef] [PubMed]

84. Smernik, R.J.; Baldock, J.A. Solid-state ^{15}N NMR analysis of highly ^{15}N-enriched plant materials. *Plant Soil* **2005**, *275*, 271–283. [CrossRef]

85. Ward, J.L.; Baker, J.M.; Beale, M.H. Recent applications of NMR spectroscopy in plant metabolomics. *FEBS J.* **2007**, *274*, 1126–1131. [CrossRef] [PubMed]

86. Faust, H. Probenchemie ^{15}N-markierter Stickstoffverbindungen im Mikro-bis Nanomolbereich für die emissionsspektrometrische Isotopenanalyse. *Isot. Environ. Health Stud.* **1967**, *3*, 100–103. [CrossRef]

87. Muhamadali, H.; Chisanga, M.; Subaihi, A.; Goodacre, R. Combining Raman and FT-IR spectroscopy with quantitative isotopic labeling for differentiation of *E. coli* cells at community and single cell levels. *Anal. Chem.* **2015**, *87*, 4578–4586. [CrossRef]

88. Iwaki, M.; Puustinen, A.; Wikstrom, M.; Rich, P.R. ATR-FTIR spectroscopy and isotope labeling of the PM intermediate of *Paracoccus denitrificans* cytochrome c oxidase. *Biochemistry* **2004**, *43*, 14370–14378. [CrossRef] [PubMed]

89. Green, L.C.; Wagner, D.A.; Glogowski, J.; Skipper, P.L.; Wishnok, J.S.; Tannenbaum, S.R. Analysis of nitrate, nitrite, and [^{15}N]-nitrate in biological fluids. *Anal. Biochem.* **1982**, *126*, 131–138. [CrossRef]

90. Dunphy, M.J.; Goble, D.D.; Smith, D.J. Nitrate analysis by capillary gas chromatography. *Anal. Biochem.* **1990**, *184*, 381–387. [CrossRef]

91. Jackson, S.J.; Siervo, M.; Persson, E.; McKenna, L.M.; Bluck, L.J. A novel derivative for the assessment of urinary and salivary nitrate using gas chromatography/mass spectrometry. *Rapid Commun. Mass Spectrom.* **2008**, *22*, 4158–4164. [CrossRef] [PubMed]

92. Gutzki, F.M.; Tsikas, D.; Alheid, U.; Frolich, J.C. Determination of endothelium-derived nitrite/nitrate by gas chromatography/tandem mass spectrometry using [^{15}N]-NaNO$_2$ as internal standard. *Biol. Mass Spectrom.* **1992**, *21*, 97–102. [CrossRef]

93. Kage, S.; Kudo, K.; Ikeda, N. Simultaneous determination of nitrate and nitrite in human plasma by gas chromatography-mass spectrometry. *J. Anal. Toxicol.* **2002**, *26*, 320–324. [CrossRef]

94. Tsikas, D.; Boger, R.H.; Bode-Boger, S.M.; Gutzki, F.M.; Frolich, J.C. Quantification of nitrite and nitrate in human urine and plasma as pentafluorobenzyl derivatives by gas chromatography-mass spectrometry using their ^{15}N-labelled analogs. *J. Chromatogr. B Biomed. Appl.* **1994**, *661*, 185–191. [CrossRef]

95. Tsikas, D.; Gutzki, F.M.; Rossa, S.; Bauer, H.; Neumann, C.; Dockendorff, K.; Sandmann, J.; Frolich, J.C. Measurement of nitrite and nitrate in biological fluids by gas chromatography-mass spectrometry and by the Griess assay: Problems with the Griess assay—Solutions by gas chromatography-mass spectrometry. *Anal. Biochem.* **1997**, *244*, 208–220. [CrossRef]

96. Hanff, E.; Eisenga, M.F.; Beckmann, B.; Bakker, S.J.; Tsikas, D. Simultaneous pentafluorobenzyl derivatization and GC-ECNICI-MS measurement of nitrite and malondialdehyde in human urine: Close positive correlation between these disparate oxidative stress biomarkers. *J. Chromatogr. B Anal. Technol. Biomed. Life Sci.* **2017**, *1043*, 167–175. [CrossRef] [PubMed]

97. Tsikas, D. Pentafluorobenzyl bromide—A versatile derivatization agent in chromatography and mass spectrometry: I. Analysis of inorganic anions and organophosphates. *J. Chromatogr. B Anal. Technol. Biomed. Life Sci.* **2017**, *1043*, 187–201. [CrossRef] [PubMed]

98. Tsikas, D. GC-ECNICI-MS/MS of eicosanoids as pentafluorobenzyl-trimethylsilyl (TMS) derivatives: Evidence of CAD-induced intramolecular TMS ether-to-ester rearrangement using carboxy-^{18}O-labelled eicosanoids and possible implications in quantitative analysis. *J. Chromatogr. B Anal. Technol. Biomed. Life Sci.* **2017**, *1047*, 185–196. [CrossRef] [PubMed]

99. Hanada, Y.; Imaizumi, I.; Kido, K.; Tanizaki, T.; Koga, M.; Shiraishi, H.; Soma, M. Application of a pentafluorobenzyl bromide derivatization method in gas chromatography/mass spectrometry of trace levels of halogenated phenols in air, water and sediment samples. *Anal. Sci.* **2002**, *18*, 655–659. [CrossRef]

100. Smith, M.T. Advances in understanding benzene health effects and susceptibility. *Annu. Rev. Public Health* **2010**, *31*, 133–148. [CrossRef]

101. Powell, G.; Johnson, F.R. Nitromesitylene. *Org. Synth.* **1934**, *14*, 68. [CrossRef]

102. Wilms, H.; Dorlars, A. Explosion resulting from the oxidation of mesitylene with nitric acid. *Angew. Chem. Int. Ed.* **1962**, *1*, 403. [CrossRef]

103. Thomas, T.D. The role of activated charcoal in plant tissue culture. *Biotechnol. Adv.* **2008**, *26*, 618–631. [CrossRef] [PubMed]

104. Mu'azu, N.D.; Jarrah, N.; Zubair, M.; Alagha, O. Removal of phenolic compounds from water using sewage sludge-based activated carbon adsorption: A review. *Int. J. Environ. Res. Public Health* **2017**, *14*, 1094. [CrossRef] [PubMed]

105. Rozhon, W.; Baubec, T.; Mayerhofer, J.; Mittelsten Scheid, O.; Jonak, C. Rapid quantification of global DNA methylation by isocratic cation exchange high-performance liquid chromatography. *Anal. Biochem.* **2008**, *375*, 354–360. [CrossRef]

106. Rozhon, W.; Kammermeier, L.; Schramm, S.; Towfique, N.; Adebimpe Adedeji, N.; Adesola Ajayi, S.; Poppenberger, B. Quantification of the pyrrolizidine alkaloid jacobine in *Crassocephalum crepidioides* by cation exchange high-performance liquid chromatography. *Phytochem. Anal.* **2018**, *29*, 48–58. [CrossRef]

107. Xu, G.; Fan, X.; Miller, A.J. Plant nitrogen assimilation and use efficiency. *Annu. Rev. Plant Biol.* **2012**, *63*, 153–182. [CrossRef] [PubMed]

108. Balazy, M.; Kaminski, P.M.; Mao, K.; Tan, J.; Wolin, M.S. S-Nitroglutathione, a product of the reaction between peroxynitrite and glutathione that generates nitric oxide. *J. Biol. Chem.* **1998**, *273*, 32009–32015. [CrossRef]

109. Go, Y.M.; Chandler, J.D.; Jones, D.P. The cysteine proteome. *Free Radic. Biol. Med.* **2015**, *84*, 227–245. [CrossRef]

110. Velioglu, Y.S.; Mazza, G.; Gao, L.; Oomah, B.D. Antioxidant activity and total phenolics in selected fruits, vegetables, and grain products. *J. Agric. Food Chem.* **1998**, *46*, 4113–4117. [CrossRef]

Sample Availability: In this study only standard chemicals were used, which are available from the sources indicated in the Materials and Methods section. Seeds of *C. crepidioides* Ilé-Ifè are available from the corresponding author.